Pentadentate Terpyridine−Catechol Linked Ligands and Their Cobalt(III) Complexes

Toshi Nagata* and Koji Tanaka

Research Center for Molecular Materials, Institute for Molecular Science, Myodaiji, Okazaki 444-8585, Japan

Received November 3, 1999

A series of novel pentadentate terpyridine−catechol linked ligands were prepared, in which the terpyridine and catechol moieties were linked together by $(CH_2)_n$ chains of different lengths (n = 4−6). Together with 1-methylimidazole, these ligands formed low-spin, six-coordinate Co(III) complexes. Two of the complexes (n = 4, 5) were characterized by X-ray crystallography [n = 4, monoclinic, $P2_1/c$, a = 14.957(7) Å, b = 10.585(9) Å, c = 23.033(7) Å, β = 106.01(3)°, V = 3505(3) Å^3, Z = 4, R = 0.063; n = 5, monoclinic, $P2_1/c$, a = 8.848(7) Å, b = 15.78(1) Å, c = 25.455(7) Å, β = 93.90(5)°, V = 3544(3) Å^3, Z = 4, R = 0.056], which revealed similar structures around the Co(III) centers but different conformations for the $(CH_2)_n$ linkers. The $(CH_2)_4$ linker showed a straight, symmetric conformation whereas the $(CH_2)_5$ linker showed a curved conformation that allowed the accommodation of one extra CH_2 unit, suggesting that the $(CH_2)_4$ linker presents the "best-fit" length for these complexes.

Introduction

Catechol is a "noninnocent" ligand with three redox forms (catecholate, semiquinonate, and quinone).[1] Metal complexes of catechol and related ligands have long been investigated,[1,2] and it is now well-known that a catecholato-derived ligand can exist as any of the three redox forms, depending on the nature of the metal and the coexisting ligands.[1,2] In some cases, valence tautomerism is observed due to the electron transfer between the metal and a ligand,[3] and such tautomerism can result in interesting physical properties such as a photomechanical effect.[3g,h] Metal−catechol interactions also have biological significance in such processes as oxidation of phenolic substrates and metal transport, which has aroused considerable interest in the field of bioinorganic chemistry.[4]

Among the metal complexes of catechols, terpyridine/catechol/metal ternary complexes are particularly promising for application in redox catalysis[5c−f] because the terpyridine ligand is expected to occupy three meridional positions in the six-coordinate octahedron, leaving the other three meridional positions for the catechol ligand and the reactive site. However, the chemistry of such ternary complexes is often complicated by ligand exchange reactions giving bis(terpyridine)metal complexes; this may explain why reports on terpyridine/catechol/metal ternary complexes have been relatively scarce.[5]

In this paper, we report the syntheses of terpyridine−catechol linked ligands, **1a**−**c**, which should improve the stability of the terpyridine/catechol/metal ternary systems and prevent formation of bis(terpyridine) complexes. We also report the syntheses and characterizations of cobalt(III) complexes of **1a**−**c**.

Results

Ligand Syntheses. The syntheses of the terpyridine−catechol linked ligands **1a**−**c** are shown in Scheme 1. In the first step, a 2-hydroxyphenyl group was introduced at the 4′-position of terpyridine via a two-step route, namely, Suzuki coupling[6] of

(1) Pierpont, C. G.; Lange, C. W. *Prog. Inorg. Chem.* **1994**, *41*, 331−442.

(2) (a) Crowley, P. J.; Haendler, H. M. *Inorg. Chem.* **1962**, *1*, 904−909. (b) Röhrscheid, F.; Balch, A. L.; Holm, R. H. *Inorg. Chem.* **1966**, *5*, 1542−1551. (c) Girgis, A. Y.; Sohn, Y. S.; Balch, A. L. *Inorg. Chem.* **1975**, *14*, 2327−2331. (d) Raymond, K. N.; Isied, S. S.; Brown, L. D.; Fronczek, F. R.; Nibert, J. H. *J. Am. Chem. Soc.* **1976**, *98*, 1767−1774. (e) Pierpont, C. G.; Downs, H. H. *J. Am. Chem. Soc.* **1976**, *98*, 4834−4838. (f) Wicklund, P. A.; Beckmann, L. S.; Brown, D. G. *Inorg. Chem.* **1976**, *15*, 1996−1997. (g) Lobanov, A. V.; Abakumov, G. A.; Razuvaev, G. A. *Dokl. Akad. Nauk SSSR* **1977**, *235*, 824−827.

(3) (a) Buchanan, R. M.; Pierpont, C. G. *J. Am. Chem. Soc.* **1980**, *102*, 4951−4957. (b) Lynch, M. W.; Hendrickson, D. N.; Fitzgerald, B. J.; Pierpont, C. G. *J. Am. Chem. Soc.* **1984**, *106*, 2041−2049. (c) Adams, D. M.; Dei, A.; Rheingold, A. L.; Hendrickson, D. N. *J. Am. Chem. Soc.* **1993**, *115*, 8221−8229. (d) Jung, O.-S.; Pierpont, C. G. *J. Am. Chem. Soc.* **1994**, *116*, 2229−2230. (e) Pierpont, C. G.; Jung, O.-S. *Inorg. Chem.* **1995**, *34*, 4281−4283. (f) Jung, O.-S.; Jo, D. H.; Lee, Y.-A.; Conklin, B. J.; Pierpont, C. G. *Inorg. Chem.* **1997**, *36*, 19−24. (g) Abakumov, G. A.; Nevodchikov, V. I. *Dokl. Akad. Nauk SSSR* **1982**, *266*, 1407−1410. (h) Lange, C. W.; Foldeaki, M.; Nevodchikov, V. I.; Cherkasov, V. K.; Abakumov, G. A.; Pierpont, C. G. *J. Am. Chem. Soc.* **1992**, *114*, 4220−4222.

(4) (a) The topics most often investigated include catechol dioxygenase models,[4b−e] tyrosinase models,[4f−i] artificial siderophores,[4j,k] and photosynthetic models.[4l,m] (b) Cox, D. D.; Que. L., Jr. *J. Am. Chem. Soc.* **1988**, *110*, 8085−8092. (c) Sheu, C.; Sobkowiak, A.; Jeoln, S.; Sawyer, D. T. *J. Am. Chem. Soc.* **1990**, *112*, 879−881. (d) Funabiki, T.; Ishikawa, M.; Nagai, Y.; Yorita, J.; Yoshida, S. *J. Chem. Soc., Chem. Commun.* **1994**, 1951−1952. (e) Simándi, L. I.; Barna, T.; Argay, G.; Simándi, T. L. *Inorg. Chem.* **1995**, *34*, 6337−6340. (f) Sorrel, T. N. *Tetrahedron* **1989**, *45*, 3−68. (g) Kitajima, N.; Koda, T.; Iwata, Y.; Moro-oka, Y. *J. Am. Chem. Soc.* **1990**, *112*, 8833−8839. (h) Paul, P. P.; Tyeklár, Z.; Jacobson, R. R.; Karlin, K. D. *J. Am. Chem. Soc.* **1991**, *113*, 5322−5332. (i) Casella, L.; Monzani, E.; Gullotti, M.; Cavagnino, D.; Cerina, G.; Santagostini, L.; Ugo, R. *Inorg. Chem.* **1996**, *35*, 7516−7525. (j) Karpishin, T. B.; Gebhard, M. S.; Solomon, E. I.; Raymond, K. N. *J. Am. Chem. Soc.* **1991**, *113*, 2977−2984. (k) Tor, Y.; Libman, J.; Shanzer, A.; Felder, C. E.; Lifson, S. *J. Am. Chem. Soc.* **1992**, *114*, 6661−6671. (l) Lynch, M. W.; Hendrickson, D. N.; Fitzgerald, B. J.; Pierpont, C. G. *J. Am. Chem. Soc.* **1984**, *106*, 2041−2049. (m) Reynolds, R. A., III; Coucouvanis, D. *Inorg. Chem.* **1998**, *37*, 170−171.

(5) (a) Folgado, J. V.; Ibanez, R.; Coronado, E.; Beltran, D.; Savariault, J. M.; Galy, J. *Inorg. Chem.* **1988**, *27*, 19−26. (b) Alonzo, G.; Consiglio, M.; Maggio, F.; Bertazzi, N. *Inorg. Chim. Acta* **1988**, *147*, 217−220. (c) Bhattacharya, S. *Polyhedron* **1994**, *13*, 451−456. (d) Kurihara, M.; Daniele, S.; Tsuge, K.; Sugimoto, H.; Tanaka, K. *Bull. Chem. Soc. Jpn.* **1998**, *71*, 867−875. (e) Sugimoto, H.; Tsuge, K.; Tanaka, K. *Chem. Lett.* **1998**, 719−720. (f) Tsuge, K.; Tanaka, K. *Chem. Lett.* **1998**, 1069−1070.

10.1021/ic9912880 CCC: $19.00
Published on Web 07/13/2000

Scheme 1

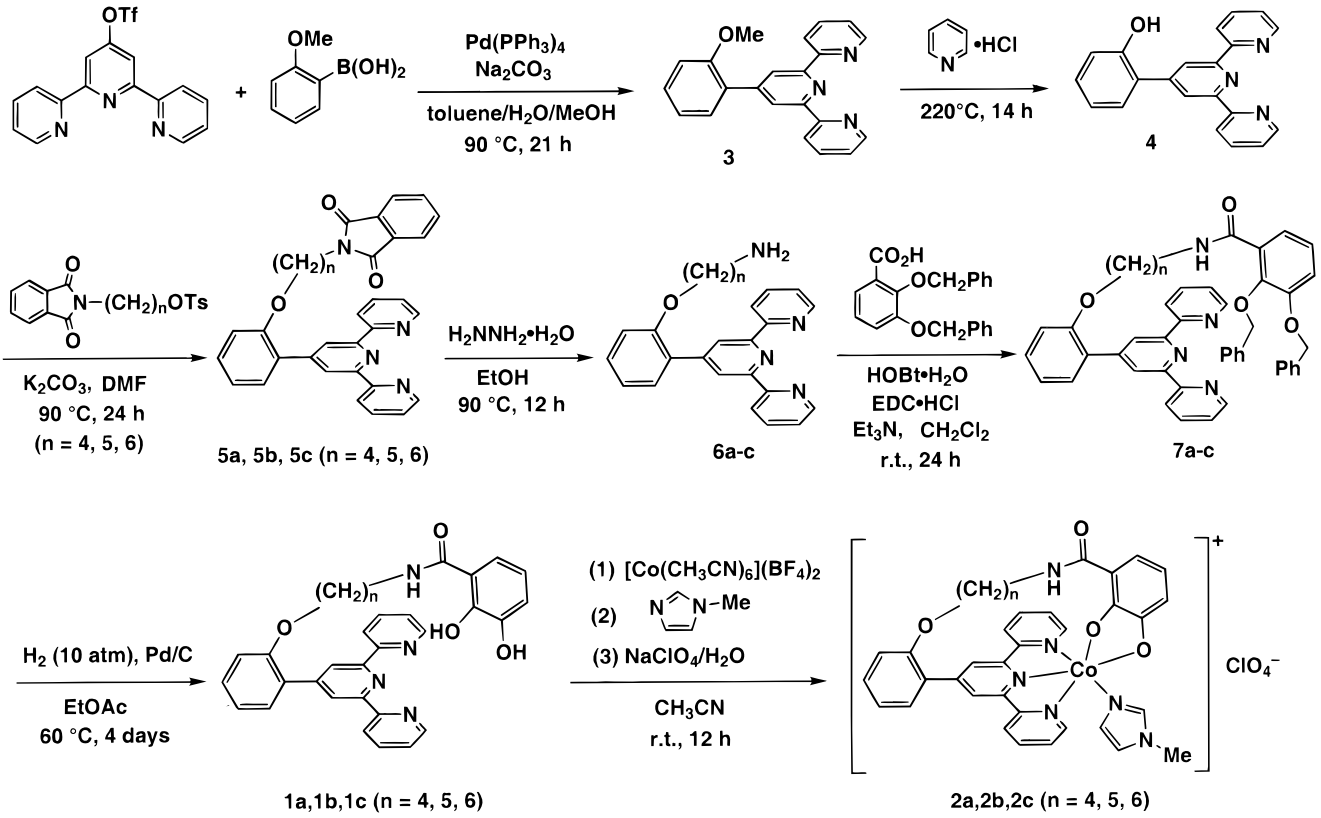

terpyridin-4′-yl triflate with 2-(methoxyphenyl)boronic acid followed by demethylation with pyridinium chloride.[7] Although the same compound (**4**) was prepared via condensation of salicylaldehyde with 2-acetylpyridine and 1-((2-pyridylcarbonyl)methyl)pyridinium iodide,[8] the present method can be a useful alternative, given the ready availability of terpyridin-4′-yl triflate[9] and higher yield at the condensation stage (which makes purification easy).

In the subsequent step, the $(CH_2)_n$ linker unit was introduced by using an ω-phthalimidoalkyl tosylate, which was prepared by fusion of phthalic anhydride and an ω-amino alcohol[10] followed by treatment with tosyl chloride. After removal of the phthalimide protecting group, the catechol moiety was introduced by condensation with 2,3-bis(benzyloxy)benzoic acid followed by hydrogenolysis of the benzyl ethers. The ligands **1a**−**c** were prepared in sufficient purity for the syntheses of the metal complexes, without need of chromatographic purification in any of the steps; they can, however, be further purified by size-exclusion HPLC when extrapure material is needed (e.g., for elemental analysis).

Syntheses of the Cobalt(III) Complexes. The cobalt(III) complexes **2a**−**c** were prepared from **1a**−**c** by treatment with $[Co(CH_3CN)_6](BF_4)_2$[11] and 1-methylimidazole (1-MeIm) under air, followed by crystallization in the presence of $NaClO_4$. The dark blue-green crystals contained one ClO_4^- anion per cobalt atom, as confirmed by elemental analysis and X-ray crystallography (see below). ^{1}H NMR spectra of CD_3CN solutions gave sharp peaks characteristic of diamagnetic complexes, indicating that the cobalt ions exist as low-spin Co(III). These results and the charge balances in the empirical formulas suggest that **2a**−**c** are best formulated as "Co(III)/catechol" complexes. The ESI-MS (electrospray ionization mass) spectra of **2a**−**c** were very similar and showed only two peaks corresponding to [Co(**1**)(1-MeIm)]$^+$ and [Co(**1**)]$^+$ cations. The latter should be a fragment peak because the integrity of each material was evident from the ^{1}H NMR spectra.

Descriptions of the Structures. The structures of **2a** and **2b** were examined by X-ray crystallography. Crystal data are listed in Table 1, selected atomic coordinates, bond lengths, and bond angles are presented in Tables 2−5, and the ORTEP[12] drawings are shown in Figure 1. The structures around the cobalt centers are very similar for the two complexes. The equatorial plane is formed by the three nitrogen atoms from terpyridine and one oxygen atom from catechol, and the axial positions are occupied by the other oxygen atom from catechol and one nitrogen atom from 1-methylimidazole. The bond lengths of the catechol rings show no evidence of bond alteration, which rules out semiquinone or quinone formulation for these rings. The coordination geometry around the Co(III) center is close to a regular octahedron; the only significant deviation is that N(1) and N(3) are pulled toward N(2) because of the small bite angles of the terpyridine ligand. In each structure, the amide

(6) Miyaura, N.; Suzuki, A. *Chem. Rev.* **1995**, *95*, 2457−2483.
(7) Green, T. W.; Wuts, P. G. M. *Protective Groups in Organic Synthesis*, 2nd ed.; John Wiley & Sons: New York, 1991; p 147.
(8) Hanabusa, K.; Nakamura, A.; Koyama, T.; Shirai, H. *Polym. Int.* **1994**, *35*, 231−238.
(9) (a) Potts, K. T.; Konwar, D. *J. Org. Chem.* **1991**, *56*, 4815−4816. (b) Constable, E. C.; Ward, M. D. *J. Chem. Soc., Dalton Trans.* **1990**, 1405−1409.
(10) (a) Turner, R. A. *J. Am. Chem. Soc.* **1953**, *75*, 2388−2390. (b) Agathocleous, D. C.; Page, P. C. B.; Cosstick, R.; Galpin, I. J.; McLennan, A. G.; Prescott, M. *Tetrahedron* **1990**, *46*, 2047−2058.
(11) (a) Hathaway, B. J.; Holah, D. G.; Underhill, A. E. *J. Chem. Soc.* **1962**, 2444−2448. (b) van Leeuwen, P. W. N. M.; Groeneveld, W. L. *Inorg. Nucl. Chem. Lett.* **1967**, *3*, 145−146.
(12) Burnett, M. N.; Johnson, C. K. *ORTEP-III*: *Oak Ridge Thermal Ellipsoid Plot Program for Crystal Structure Illustrations*; Report ORNL-6895; Oak Ridge National Laboratory: Oak Ridge, TN, 1996.

Table 1. Crystallographic Parameters for **2a** and **2b**

	2a·H_2O	**2b**·H_2O
formula	$C_{36}H_{34}N_6O_9ClCo$	$C_{37}H_{36}N_6O_9ClCo$
fw	789.09	803.11
crystal size (mm)	0.50 × 0.30 × 0.20	0.50 × 0.50 × 0.50
system	monoclinic	monoclinic
space group	$P2_1/c$	$P2_1/c$
a (Å)	14.957(7)	8.848(7)
b (Å)	10.585(9)	15.78(1)
c (Å)	23.033(7)	25.455(7)
β (deg)	106.01(3)	93.90(5)
V (Å^3)	3505(3)	3544(3)
D_x (g cm^{-3})	1.495	1.505
Z	4	4
T (K)	296	296
no. of reflns	8805	9076
no. of obsd reflns ($I > 3\sigma(I)$)	4048	3446
no. of variables	487	481
μ(Mo Kα) (cm^{-1})	6.31	6.26
F(000)	1632	1664
scan width (deg)	1.00 + 0.30 tan θ	1.00 + 0.30 tan θ
$2\theta_{max}$ (deg)	55	55
2θ range of reflns for cell parameter determination (deg)	20−23	20−25
max peak (e Å^{-3})	0.78	0.79
min peak (e Å^{-3})	−0.62	−0.63
R^a	0.063	0.056
$R_w{}^a$	0.061	0.053

[a] $R = \sum||F_o| - |F_c||/\sum|F_o|$; $R_w = [\sum w(|F_o| - |F_c|)^2/\sum wF_o^2]^{1/2}$ ($w = 1/\sigma^2(F_o^2)$). R and R_w were calculated for observed reflections.

Table 2. Selected Atomic Coordinates and Equivalent Isotropic Thermal Parameters (Å^2) for **2a**

atom	x	y	z	B_{eq}
Co(1)	0.28532(6)	0.10346(9)	0.93895(4)	3.00(2)
O(1)	0.2085(3)	−0.0079(4)	0.9673(2)	3.3(1)
O(2)	0.3765(3)	0.0767(4)	1.0127(2)	3.9(1)
N(1)	0.2247(3)	0.2472(5)	0.9646(2)	3.2(1)
N(2)	0.1870(3)	0.1198(5)	0.8686(2)	2.7(1)
N(3)	0.3203(3)	−0.0331(5)	0.8939(2)	3.3(1)
N(4)	0.0652(4)	−0.1350(6)	0.9828(3)	3.8(1)

Table 3. Selected Bond Lengths (Å) and Bond Angles (deg) for **2a**

Co(1)−O(1)	1.884(4)	Co(1)−O(2)	1.883(4)
Co(1)−N(1)	1.945(5)	Co(1)−N(2)	1.872(5)
Co(1)−N(3)	1.933(5)	Co(1)−N(5)	1.927(5)
O(1)−Co(1)−O(2)	87.3(2)	O(1)−Co(1)−N(1)	90.2(2)
O(1)−Co(1)−N(2)	87.1(2)	O(1)−Co(1)−N(3)	89.9(2)
O(1)−Co(1)−N(5)	177.4(2)	O(2)−Co(1)−N(1)	97.3(2)
O(2)−Co(1)−N(2)	174.4(2)	O(2)−Co(1)−N(3)	97.8(2)
O(2)−Co(1)−N(5)	90.2(2)	N(1)−Co(1)−N(2)	82.5(2)
N(1)−Co(1)−N(3)	164.9(2)	N(1)−Co(1)−N(5)	90.6(2)
N(2)−Co(1)−N(3)	82.5(2)	N(2)−Co(1)−N(5)	95.5(2)
N(3)−Co(1)−N(5)	89.9(2)		

NH bond (N(4)−H(1)) points toward the "axial" oxygen atom (O(1)) to form an intramolecular hydrogen bond (N(4)···O(1) distances are 2.638(7) and 2.675(6) Å for **2a** and **2b**, respectively).

Figure 2 shows alternative diagrams of **2a** and **2b** viewed along the "axial" directions. The two structures have different orientations for the $(CH_2)_n$ linkers. The $(CH_2)_4$ linker in **2a** (Figure 2a) runs straight along the approximate mirror plane that contains the catechol ring and bisects the terpyridine ligand, whereas the $(CH_2)_5$ linker in **2b** (Figure 2b) forms a curved conformation. Also markedly different are the dihedral angles between the central ring of terpyridine and the phenyl group bearing the $(CH_2)_n$ linker (**2a**, 79.9°; **2b**, 45.2°). Since the local structures around the Co(III) center are very similar for the two

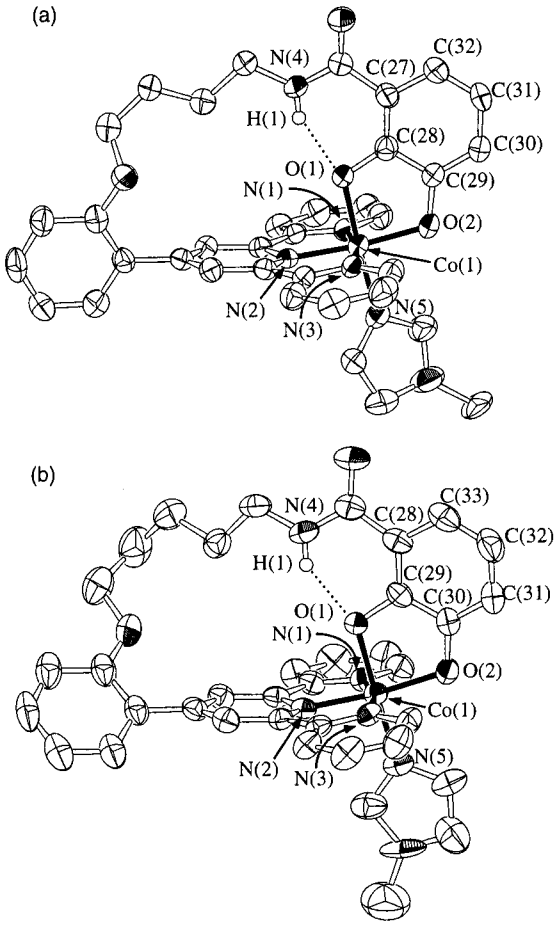

Figure 1. ORTEP views (50% probability ellipsoids) of the complex cations in (a) **2a** and (b) **2b**. The dotted lines indicate intramolecular hydrogen bonds.

Table 4. Selected Atomic Coordinates and Equivalent Isotropic Thermal Parameters (Å^2) for **2b**

atom	x	y	z	B_{eq}
Co(1)	0.90308(9)	0.09150(5)	0.32393(3)	2.91(2)
O(1)	1.0061(4)	0.0407(2)	0.3830(1)	3.2(1)
O(2)	0.9188(4)	−0.0131(3)	0.2889(1)	3.6(1)
N(1)	1.0924(5)	0.1453(3)	0.3083(2)	3.2(1)
N(2)	0.8895(5)	0.1866(3)	0.3667(2)	2.9(1)
N(3)	0.7060(5)	0.0662(3)	0.3497(2)	3.1(1)
N(4)	1.1602(6)	0.0097(4)	0.4751(2)	3.9(1)

Table 5. Selected Bond Lengths (Å) and Bond Angles (deg) for **2b**

Co(1)−O(1)	1.884(4)	Co(1)−O(2)	1.886(4)
Co(1)−N(1)	1.943(5)	Co(1)−N(2)	1.862(5)
Co(1)−N(3)	1.946(5)	Co(1)−N(5)	1.919(5)
O(1)−Co(1)−O(2)	87.6(2)	O(1)−Co(1)−N(1)	88.5(2)
O(1)−Co(1)−N(2)	85.6(2)	O(1)−Co(1)−N(3)	92.3(2)
O(1)−Co(1)−N(5)	178.2(2)	O(2)−Co(1)−N(1)	101.1(2)
O(2)−Co(1)−N(2)	172.5(2)	O(2)−Co(1)−N(3)	94.4(2)
O(2)−Co(1)−N(5)	90.7(2)	N(1)−Co(1)−N(2)	81.9(2)
N(1)−Co(1)−N(3)	164.5(2)	N(1)−Co(1)−N(5)	91.1(2)
N(2)−Co(1)−N(3)	82.7(2)	N(2)−Co(1)−N(5)	96.1(2)
N(3)−Co(1)−N(5)	88.7(2)		

complexes, the structural difference is mainly due to the different lengths of the polymethylene linkers; the $(CH_2)_4$ linker presents the "best-fit" length, while the $(CH_2)_5$ linker has to curve to accommodate the extra CH_2 unit.

In each case, the central ring of terpyridine is noticeably bent out of the equatorial plane; the dihedral angles are 13.1 and 15.5° for **2a** and **2b**, respectively. These angles are quite unusual

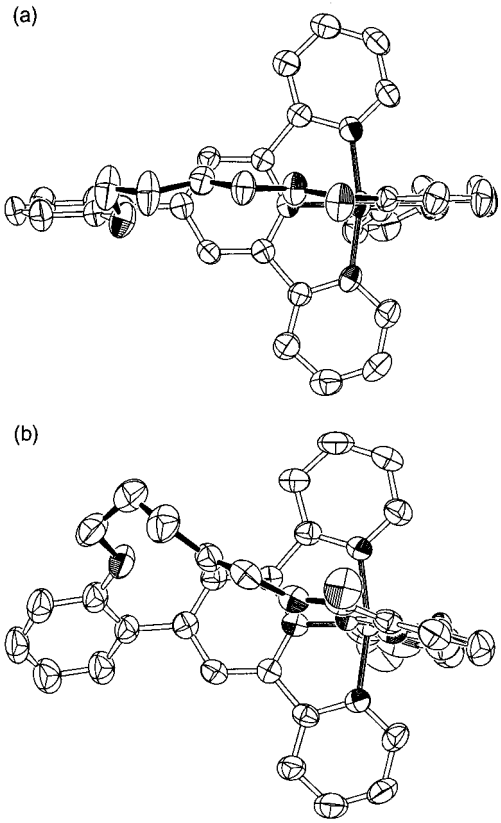

Figure 2. ORTEP diagrams of the complex cations in (a) **2a** and (b) **2b** viewed down the O(1)−Co(1) bond. The $(CH_2)_n$ linkers are shown by filled bonds.

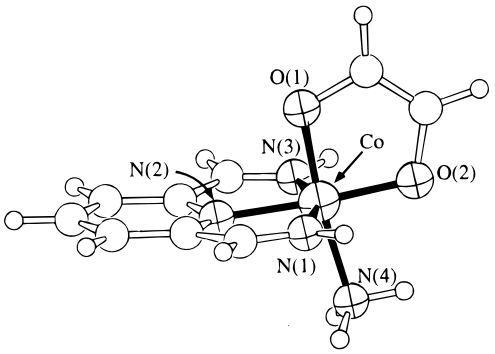

Figure 3. Optimized structure of the [Co(2,6-pyridinedicarboxaldimine)(1,2-ethenediolato(2−))(NH_3)]$^+$ cation, a model system for **2a**−**c**, derived from quantum chemical computations.

for Co−terpyridine complexes (typical values are 2−4° for both Co(II) and Co(III) terpyridine complexes[13]). This anomaly cannot be explained by the effect of the polymethylene linkers because the structures of the Co−terpyridine components are very similar for **2a** and **2b**, despite the different linker lengths and very different structures of the polymethylene components in these complexes (see above). Therefore, we propose that the anomaly is caused by electronic and/or crystal packing effects. Quantum chemical computations suggest that electronic effects are important. Figure 3 shows the optimized structure of the cation [Co(2,6-pyridinedicarboxaldimine)(1,2-ethenediolato(2−)(NH_3)]$^+$ derived from ab initio calculations. The pyridine ring is bent out of the equatorial plane by 10.5°. The calculated structure is remarkably similar to the X-ray structures of **2a** and **2b**, indicating that electronic interactions are largely responsible for the bent structure.

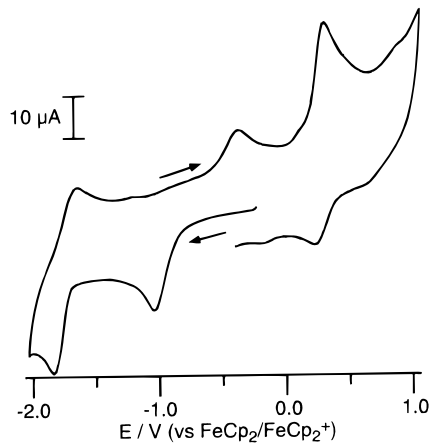

Figure 4. Cyclic voltammogram of **2c**. Conditions: 1.5 mM solution in CH_3CN containing 0.1 M Bu_4NClO_4; Pt working and counter electrodes; scan rate 1.0 V/s; at room temperature under N_2.

Electrochemistry and Absorption Spectra. The cyclic voltammogram of **2c** in CH_3CN is shown in Figure 4. The reversible wave at −1.8 V (vs the ferrocene/ferrocenium couple) corresponds to the terpyridine/terpyridine$^{\bullet-}$ redox couple. The cathodic peak at −1.0 V and the anodic peak at −0.3 V correspond to the Co(III)/Co(II) redox couple. The partially reversible wave at +0.4 V corresponds to oxidation of the catechol ligand. Complexes **2a** and **2b** showed essentially the same voltammograms.

To rationalize the large peak-to-peak separation and poor reversibility of the Co(III)/Co(II) couple, we examined the effects of scan rates and addition of excess 1-methylimidazole (Figure 5). At a slower scan speed and without an additive (Figure 5a, left), the peak potentials shifted on repeated scans and the anodic current was apparently smaller than the cathodic current. On addition of 100 equiv of 1-methylimidazole (Figure 5b, left), the shift of peak potentials was suppressed and the anodic current recovered to match the cathodic current. The peak-to-peak separation was also much smaller, and the overall voltammogram appeared more like a reversible one. The irreversibility of this redox couple was therefore caused, at least partly, by dissociation of the 1-methylimidazole ligand. It should be noted, however, that even in the presence of excess 1-methylimidazole (Figure 5b, right), the peak-to-peak separation became larger again at a faster scan rate. This behavior is typically observed when electron transfer between an electrode and a metal complex is slow (i.e., a non-Nernstian or electrochemically irreversible process).[14] This slow electron transfer is most likely caused by the large internal reorganization energy due to the structural difference between the Co(III) and Co(II) states.[15]

The electronic spectra of **2a**−**c** in CH_3CN solutions showed only weak peaks in the 500−2000 nm range. For samples in

(13) (a) Maslan, E. N.; Raston, C. L.; White, A. H. *J. Chem. Soc., Dalton Trans.* **1974**, 1803−1807. (b) Raston, C. L.; White, A. H. *J. Chem. Soc., Dalton Trans.* **1976**, 7−12. (c) Kucharski, E. S.; Skelton, B. W.; White, A. H. *Aust. J. Chem.* **1978**, *31*, 47−51. (d) Kepert, D. L.; Kucharski, E. S.; White, A. H. *J. Chem. Soc., Dalton Trans.* **1980**, 1932−1938. (e) Corey, E. J.; Cooper, N. J.; Canning, W. M.; Lipscomb, W. N.; Koetzle, T. F. *Inorg. Chem.* **1982**, *21*, 192−199. (f) Henke, W.; Kremer, S. *Inorg. Chim. Acta* **1982**, *65*, L115−L117. (g) Takusagawa, F.; Yohannes, P. G.; Mertes, K. B. *Inorg. Chim. Acta* **1986**, *114*, 165−169. (h) Jitsukawa, K.; Hata, T.; Yamamoto, T.; Kano, K.; Masuda, H.; Einaga, H. *Chem. Lett.* **1994**, 1169−1172. (i) Ramprasad, D.; Gilicinski, A. G.; Markley, T. J.; Pez, G. P. *Inorg. Chem.* **1994**, *33*, 2841−2847.

(14) Astruc, D. *Transition-Metal Chemistry*; VCH: New York, 1995; pp 96−99.

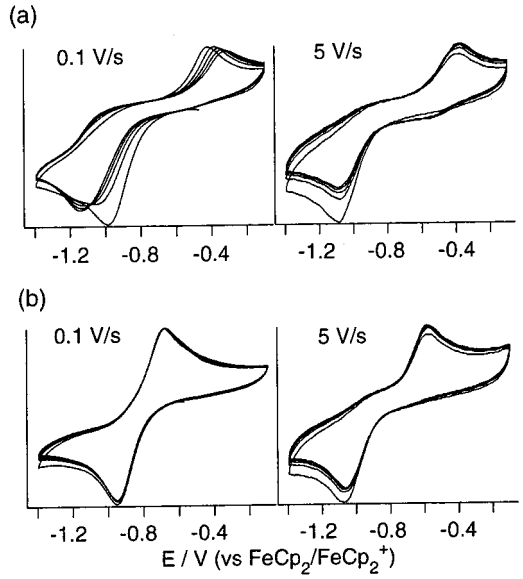

Figure 5. Cyclic voltammograms of **2c**: (a) 10 repeated scans under the same conditions as those for Figure 4 except for the scan rates; (b) 10 repeaed scans with addition of 100 equiv of 1-methylimidazole.

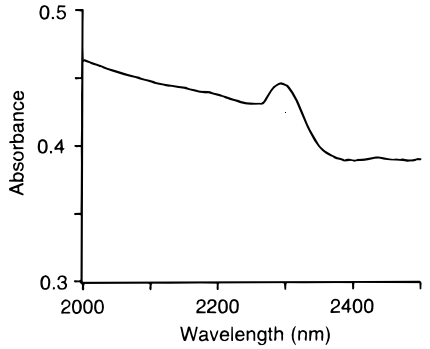

Figure 6. Near-IR absorption spectrum of **2a** in a KBr pellet (0.70 mg of **2a** in 70 mg of KBr; 13 mm diameter).

KBr pellets, a characteristic peak was observed at 2290 nm (Figure 6). Although this peak also quite weak, its location matches with those observed for other Co(III)−catechol complexes reported by Pierpont.[3d−f] Therefore, we tentatively assign this peak as a catechol → Co(III) charge-transfer transition.[16]

Discussion

Syntheses. Although terpyridine ligands with catechol or hydroquinone substituents were reported previously,[17] they had the substituents at the 4′-positions of the terpyridines, either attached directly[17a−c] or attached via a 1,4-phenylene spacer,[17d,e] which did not allow direct interactions between the substituents and the metal ions bound to the terpyridine ligands. Our ligands **1a**−**c** are, to the best of our knowledge, the first examples of catechol-terpyridine linked compounds that allow simultaneous binding of both moieties to a single metal ion.[18] The general synthesis is simple and straightforward, with no need of time-consuming chromatographic purification. The catechol moiety is connected via an amide linkage, which allows formation of an intramolecular hydrogen bond between the amide NH and one of the catechol oxygen atoms. This structural feature is shared by metal complexes of natural and artificial siderophores (enterobactin[19a] and related artificial tris(catecholamide) ligands[19b]) and provides additional stability of the metal complexes. The amide linkage is also convenient from the synthetic point of view because it can be easily formed by the carbodiimide coupling reaction, which requires simple procedures and proceeds cleanly under mild conditions. Despite the presence of flexible methylene linkers that potentially allow formation of polynuclear complexes, the isolated yields of the mononuclear cobalt(III) complexes **2a**−**c** were fairly good (50−60%).

Structures of the Co(III) Complexes. The X-ray structures of **2a** and **2b** revealed several noteworthy features. First, the intramolecular hydrogen bonds described above were indeed present. Second, the conformations of the $(CH_2)_n$ linkers were very different in **2a** and **2b**, suggesting the $(CH_2)_4$ linker in **2a** fits better than the longer linker in **2b**. Third, despite the different conformations of the linkers, the coordination geometries around the cobalt centers were very similar for the two complexes. Fourth, the central pyridine rings of the terpyridine ligands are bent out of the equatorial planes.

The last feature is ascribed to electronic effects (see Figure 3). Although the exact nature of the electronic effects is still unclear, the presence of an anionic phenolato (or enolato, in the case of the model system for computations) oxygen at the axial position seems important, as suggested by the following computational results. The 1,2-ethenediolato(2−) ligand in Figure 3 was replaced with a glycolaldehyde anion (O═CH−CH_2O^-), and the structures of the two stereoisomers (one has the alcoholato(1−) oxygen at the axial position, and the other has it in an equatorial position) were optimized. The results (Supporting Information, Figure B) showed a marked difference; the isomer with an axial alcoholato oxygen had much greater deviation from coplanarity than the isomer with an equatorial alcoholato oxygen (the dihedral angles between the pyridine ring planes and the cobalt equatorial planes were 12.5 and 5.8°, respectively). This is an interesting and unprecedented phenomenon in Co(terpyridine) chemistry and will be worth further investigation.

Comparison of the structures of **2a** and **2b** suggests that the $(CH_2)_4$ chain presents the best-fit length between the phenyl and the catechol rings. On the other hand, it is interesting to note that a longer chain with *two* extra CH_2 groups in **2c** can also accommodate itself in the same space (i.e., between the phenyl and the catechol rings). Although we have not yet determined the X-ray structure of **2c**, we assume that it is structurally similar to **2a** and **2b**, as the spectral properties (particularly ESI-MS and ^{1}H NMR) of these compounds were very similar. A longer chain allows more flexibility, which can

(15) Cotton, F. A.; Wilkinson, G. *Advanced Inorganic Chemistry*, 5th ed.; Wiley: New York, 1988; p 1309.

(16) Another possibility is that this band (2290 nm = 4367 cm^{-1}) is an overtone of a vibrational band at either 2183 cm^{-1} (2183 = 4367/2) or 1456 cm^{-1} (1456 = 4367/3). This seems unlikely, however, because the IR spectrum recorded under the same conditions revealed that there are no bands near 2183 cm^{-1} and that the bands around 1450 cm^{-1} are not particularly strong.

(17) (a) Howard, C.; Ward, M. D. *Angew. Chem., Int. Ed. Engl.* **1992**, *31*, 1028−1030. (b) Whittle, B.; Everest, N. S.; Howard, C.; Ward, M. D. *Inorg. Chem.* **1995**, *34*, 2025−2032. (c) Storrier, G. D.; Cikvrabm, S. B. *J. Chem. Soc., Dalton Trans.* **1996**, 2185−2186. (d) Storrier, G. D.; Colbran, S. B.; Craig, D. C. *J. Chem. Soc., Dalton Trans.* **1997**, 3011−3028. (e) Storrier, G. D.; Colbran, S. B.; Craig, D. C. *J. Chem. Soc., Dalton Trans.* **1998**, 1351−1363.

(18) (a) Lacour and co-workers reported[18b] a trinucleating catechol ligand that has two piperazine groups attached to one catechol ring, but this ligand was designed for the catechol ring to bridge two metal ions, rather than to chelate to a single metal ion. (b) Gojon, E.; Gaillard, J.; Latour, J.-M.; Laugier, J. *Inorg. Chem.* **1987**, *26*, 2046−2052.

(19) (a) Karpishin, T. B.; Raymond, K. N. *Angew. Chem., Int. Ed. Engl.* **1992**, *31*, 466−468. (b) McMurry, T. J.; Hosseini, M. W.; Garrett, T. M.; Hahn, F. E.; Reyes, Z. E.; Raymond, K. N. *J. Am. Chem. Soc.* **1987**, *109*, 7196−7198.

be important in chemical reactions. Our next goal will be to utilize these unique ligands for controlling chemical reactivity of the metal complexes.

Experimental Section

General Information. All reagents and solvents were of commercial reagent grade and were used without further purification unless otherwise noted. TLC analyses were performed with Merck Kieselgel 60 F_{254} (silica gel) and aluminum oxide 60 F_{254} (neutral alumina) precoated sheets. ^{1}H NMR spectra were recorded on a JEOL Lambda-500 (500 MHz) spectrometer, and chemical shifts are reported on the δ scale relative to Me_4Si in ppm. IR spectra were recorded on a Shimadzu FTIR-8300 spectrometer. Preparative HPLC was performed on a model LC-908 chromatograph (Japan Analytical Industry) equipped with JAIGEL-1H and -2H polystyrene size-exclusion columns (exclusion limits ca. 1000 and 5000 dalton, respectively). Elemental analyses were obtained on a Yanaco MT-3 analyzer. High-resolution FAB-MS spectra were recorded on a JEOL HX-110 mass spectrometer (CH_2Cl_2/3-nitrobenzyl alcohol matrix) at Kyoto University, and electrospray ionization mass (ESI-MS) spectra were obtained on a Perkin-Elmer SCIEX API-300 mass spectrometer. Cyclic voltammetry was performed with an ALS model 660 electrochemical analyzer, and electronic absorption spectra were recorded on a Shimadzu UV-3100PC spectrometer.

Ligand Syntheses. 4′-(2-Methoxyphenyl)-2,2′:6′,2″-terpyridine (3). A mixture of 4′-((trifluoromethanesulfonyl)oxy)-2,2′:6′,2″-terpyridine[9] (4.77 g, 12.8 mmol), (2-methoxyphenyl)boronic acid[20] (1.94 g, 12.8 mmol), Na_2CO_3 (2.72 g, 25.6 mmol), $Pd(PPh_3)_4$ (151 mg, 0.13 mmol), toluene (30 mmol), water (12 mL), and methanol (12 mL) was purged with Ar and heated to 90 °C for 15 h under an Ar stream. $Pd(PPh_3)_4$ (50 mg) was added, and the mixture was further heated to 90 °C for 6 h. The organic layer was then separated from the mixture, and the aqueous layer was extracted with toluene. The combined organic material was dried over Na_2SO_4 and evaporated. Dissolving the resulting orange oil in EtOH and addition of hexane gave pale yellow crystals, which were collected and washed with hexane. Yield: 2.20 g (6.48 mmol, 51%). Mp: 129−130 °C (EtOH). ^{1}H NMR ($CDCl_3$), δ: 8.71 (2H, dt, J = 5 Hz, 1 Hz), 8.67 (2H, d, J = 8 Hz), 8.63 (2H, s), 7.87 (2H, td, J = 7 Hz, 2 Hz), 7.53 (1H, dd, J = 8 Hz, 2 Hz), 7.39 (1H, td, J = 8 Hz, 2 Hz), 7.33 (2H, dd, J = 7 Hz, 5 Hz), 7.07 (1H, t, J = 7 Hz), 7.02 (1H, d, J = 8 Hz), 3.86 (3H, s). Anal. Calcd for $C_{22}H_{17}N_5O$: C, 77.86; H, 5.05; N, 12.38. Found: C, 78.16; H, 4.84; N, 12.42.

4′-(2-Hydroxyphenyl)-2,2′:6′,2″-terpyridine (4). A mixture of **3** (2.00 g, 5.89 mmol) and pyridinium chloride (10.0 g, 86.5 mmol) was purged with Ar and heated to 220 °C for 12 h. The mixture was gently evacuated to remove the generated pyridine, and heating was continued for 2 h. After the mixture was allowed to cool to room temperature, water (20 mL) was added and the pH was adjusted to 7 with 5% aqueous NH_3. The pale violet precipitate was collected and washed with water. This crude material was suspended in 10 mL of EtOH, and the suspension was heated to 100 °C for 10 min and cooled. Et_2O (20 mL) was added, and the pale pink precipitate was collected, washed with Et_2O, and dried in a vacuum. Yield: 1.76 g (5.41 mmol, 92%). Mp: 257−259 °C (EtOH). ^{1}H NMR (DMSO-d_6), δ: 10.02 (1H, s), 8.80 (2H, d, J = 5 Hz), 8.75 (2H, s), 8.73 (2H, d, J = 8 Hz), 8.09 (2H, t, J = 8 Hz), 7.57 (3H, dd + d), 7.38 (1H, t, J = 8 Hz), 7.11 (1H, dd, J = 8 Hz, 2 Hz), 7.06 (1H, t, J = 8 Hz). Anal. Calcd for $C_{21}H_{15}N_3O$: C, 77.52; H, 4.65; N, 12.91. Found: C, 77.66; H, 4.34; N, 12.91.

4-Phthalimido-1-butanol. 4-Amino-1-butanol (1.78 g, 20 mmol) and phthalic anhydride (2.96 g, 20 mmol) were fused at 160 °C for 15 min, and the mixture was evacuated for 15 min to remove the generated water. The mixture was cooled and dissolved in CH_2Cl_2. The solution was washed with 0.5 N HCl and saturated $NaHCO_3$, dried over Na_2SO_4, and evaporated. The residual oil solidified on standing. Yield: 3.35 g (15.3 mmol, 76%). Mp: 54−55 °C (Et_2O/hexane; lit.[21] 57−59 °C). ^{1}H NMR ($CDCl_3$), δ: 7.84 (2H, m), 7.72 (2H, m), 3.75 (2H, t, J = 8 Hz), 3.70 (2H, t, J = 6 Hz), 1.79 (2H, m), 1.62 (2H, m), 1.45 (broad).

4-Phthalimidobutyl 4-Toluenesulfonate. 4-Phthalimido-1-butanol (658 mg, 3.0 mmol) and 4-toluenesulfonyl chloride (629 mg, 3.3 mmol) were separately dissolved in dry pyridine (each 1 mL), and the two solutions were combined at 0 °C. The mixture was kept at 4 °C for 12 h; colorless crystals of pyridinium chloride formed. The mixture was then poured into 60 mL of 1 N HCl containing 20 g of ice. An oily product formed and then solidified on stirring. The solid was collected by filtration, washed with water, and dissolved in CH_2Cl_2, and the solution was dried over Na_2SO_4. Evaporating the solvent gave a pale yellow oil, which again solidified upon evacuation at 1 mmHg. Yield: 962 mg (2.58 mmol, 86%). Mp: 109−110 °C (CH_2Cl_2/hexane). ^{1}H NMR ($CDCl_3$), δ: 7.83 (2H, m), 7.78 (2H, d, J = 8 Hz), 7.71 (2H, m), 7.33 (2H, d, J = 8 Hz), 4.06 (2H, t, J = 6 Hz), 3.65 (2H, t, J = 6 Hz), 2.44 (3H, s), 1.70 (4H, m).

4′-(2-((4-Phthalimidobutyl)oxy)phenyl)-2,2′:6′,2″-terpyridine (5a). A mixture of **4** (651 mg, 2.0 mmol), 4-phthalimidobutyl 4-toluenesulfonate (822 mg, 2.2 mmol), and K_2CO_3 (1.11 g, 8.0 mmol) in dry DMF (10 mL) was heated to 90 °C under Ar for 12 h. The solvent was distilled off under reduced pressure, and water (30 mL) was added to the residue. The mixture was extracted with CH_2Cl_2, dried over Na_2SO_4, and evaporated. [Note: The extraction step is often hampered by formation of emulsion. Using a centrifuge is recommended. Alternatively, avoid vigorous shaking on first addition of CH_2Cl_2 but separate the organic layer after swinging the separatory funnel gently; this should transfer most of the product into the organic layer, and subsequent extraction should be much easier.] The resulting pale brown oil was dispersed in 8 mL of EtOH, and the dispersion was heated to 90 °C to give solid material; water (8 mL) was added while hot, and the mixture was slowly cooled to room temperature. The pale brown powder was collected by filtration, washed with water, and dried in a vacuum. Yield: 965 mg (1.83 mmol, 92%). Mp: 149−150 °C (EtOH). ^{1}H NMR ($CDCl_3$), δ: 8.69 (2H, s), 8.66 (4H, m), 7.84 (2H, t, J = 6 Hz), 7.79 (2H, m), 7.70 (2H, m), 7.57 (1H, dd, J = 7 Hz, 2 Hz), 7.37 (1H, td, J = 7 Hz, 2 Hz), 7.27 (2H, m), 7.07 (1H, t, J = 8 Hz), 7.01 (1H, d, J = 8 Hz), 4.08 (2H, t, J = 6 Hz), 3.62 (2H, t, J = 7 Hz), 1.87 (2H, m), 1.78 (2H, m). Anal. Calcd for $C_{33}H_{26}N_4O_3$: C, 75.27; H, 4.98; N, 10.64. Found: C, 75.42; H, 4.72; N, 10.58.

4′-(2-((4-Aminobutyl)oxy)phenyl)-2,2′:6′,2″-terpyridine (6a). Compound **5a** (891 mg, 1.69 mmol) was suspended in 12 mL of EtOH, $H_2NNH_2{\cdot}H_2O$ (423 mg, 8.45 mmol) was added, and the mixture was heated to 90 °C under Ar for 12 h. The initial suspension became a clear solution on heating; then a white solid precipitated. After the mixture was cooled to room temperature, the white solid was filtered off, and the filtrate was evaporated to give a pale brown oil. This oil was dissolved in CH_2Cl_2, and the solution was washed twice with water, dried over Na_2SO_4, and evaporated to give a colorless waxy solid. Yield: 656 mg (1.65 mmol, 98%). ^{1}H NMR ($CDCl_3$), δ: 8.70 (2H, m), 8.69 (2H, s), 8.67 (2H, d, J = 7 Hz), 7.87 (2H, td, J = 7 Hz, 2 Hz), 7.57 (1H, dd, J = 8 Hz, 2 Hz), 7.37 (1H, td, J = 7 Hz, 2 Hz), 7.33 (2H, dd, J = 7 Hz, 5 Hz), 7.06 (1H, t, J = 7 Hz), 7.00 (1H, d, J = 9 Hz), 4.04 (2H, t, J = 6 Hz), 2.60 (2H, t, J = 7 Hz), 1.77 (2H, m), 1.59 (2H, m). FAB-MS, m/z: = 397.208 ($M + H^+$); calcd for $C_{25}H_{25}N_4O$, 397.203.

4′-(2-((4-(2,3-Bis(benzyloxy)benzamido)butyl)oxy)phenyl)-2,2′:6′,2″-terpyridine (7a). Compound **6a** (588 mg, 1.48 mmol), 2,3-bis(benzyloxy)benzoic acid[22] (495 mg, 1.48 mmol), triethylamine (0.21 mL, 1.48 mmol), 1-hydroxybenzotriazole monohydrate (227 mg, 1.48 mmol), and 1-(3-(dimethylamino)propyl)-3-ethylcarbodiimide hydrochloride (284 mg, 1.48 mmol) were mixed in 30 mL of CH_2Cl_2, and the resulting solution was stirred for 24 h at room temperature under Ar. The reaction mixture was then washed twice with water. (Note: Neutral water is sufficient to remove the byproducts; use of dilute acid may result in a purple product. The washed mixture was dried over Na_2SO_4 and evaporated to give a colorless foamy material. Yield: 981 mg (1.38 mmol, 93%). ^{1}H NMR ($CDCl_3$), δ: 8.69 (2H, s), 8.62 (4H, m), 7.80 (2H, td, J = 8 Hz, 2 Hz), 7.78 (1H, t, J = 6 Hz), 7.67 (1H,

(20) Bolm, C.; Ewald, M.; Felder, M.; Schlingloff, G. *Chem. Ber.* **1992**, *125*, 1169−1190.
(21) Sugiura, S.; Inoue, S.; Hayashi, Y.; Kishi, Y.; Goto, T. *Tetrahedron* **1969**, *25*, 5155−5161.
(22) Deng, J. G.; Hamada, Y.; Shioiri, T. *Synthesis* **1998** (special issue), 627−638.

m), 7.58 (1H, dd, J = 8 Hz, 2 Hz), 7.45 (2H, d, J = 7 Hz), 7.37 (4H, m), 7.24 (4H, m), 7.18 (3H, m), 7.13 (2H, m), 7.07 (1H, t, J = 8 Hz), 6.96 (1H, d, J = 8 Hz), 5.14 (2H, s), 4.98 (2H, s), 3.91 (2H, t, J = 6 Hz), 3.21 (2H, q, J = 6 Hz), 1.63 (2H, m), 1.51 (2H, m). FAB-MS, m/z: = 713.319 (M + H^+); calcd for $C_{46}H_{41}N_4O_4$, 713.313.

4′-(2-((4-(2,3-Dihydroxybenzamido)butyl)oxy)phenyl)-2,2′:6′,2″-terpyridine (1a). Compound **7a** (902 mg, 1.27 mmol) was dissolved in 30 mL of ethyl acetate, and 10% Pd/C (230 mg) was added. The mixture was placed in a stainless steel bomb and treated with 10 atm (1 atm = 0.1013 MPa) of H_2 at 60 °C. The reaction was monitored every 24 h by TLC (alumina, CH_2Cl_2/MeOH (v/v) = 100/5); if the starting material (R_f = 1.0) or the intermediate (R_f = 0.2−0.5) was detected, the reaction was continued after addition of Pd/C (50 mg). The catalyst was filtered off, and the filtrate was evaporated to give a colorless oil, which gradually solidified upon trituration in CH_2Cl_2/hexane. Yield: 567 mg (1.06 mmol, 83%). This material was sufficiently pure for synthesis of the cobalt complexes. An analytical sample was purified by preparative HPLC followed by recrystallization from EtOH/hexane. Mp: 134−135 °C (EtOH/hexane). ^{1}H NMR ($CDCl_3$), δ: 12.75 (broad), 8.69 (2H, s), 8.65 (2H, d, J = 6 Hz), 8.63 (2H, d, J = 8 Hz), 7.86 (2H, td, J = 8 Hz, 2 Hz), 7.56 (1H, dd, J = 8 Hz, 2 Hz), 7.38 (1H, td, J = 8 Hz, 2 Hz), 7.31 (2H, dd, J = 6 Hz, 5 Hz), 7.08 (1H, t, J = 7 Hz), 7.02 (1H, d, J = 8 Hz), 6.90 (1H, dd, J = 5 Hz, 4 Hz), 1.63 (1H, br), 6.48 (2H, m), 5.8 (very broad), 4.10 (2H, t, J = 5 Hz), 3.43 (2H, q, J = 6 Hz), 1.87 (4H, m). Anal. Calcd for $C_{34}H_{32}N_4O_4$: C, 72.84; H, 5.75, N, 9.99. Found: C, 72.61; H, 5.96; N, 9.77.

Complex Syntheses. *Caution!* Organic perchlorate salts are potentially explosive. Although we experienced no accidents, all compounds containing perchlorate should be handled with care and in small amounts.

[Co(1a)(1-MeIm)]ClO_4 (2a). To a suspension of **1a** (135 mg, 0.25 mmol) in 10 mL of CH_3CN was added a solution of $[Co(CH_3CN)_6](BF_4)_2$[11] (120 mg, 0.25 mmol) in 10 mL of CH_3CN. To the resulting orange-brown solution was added 1-methylimidazole (1-MeIm; 0.12 mL, 1.5 mmol), and the mixture was stirred under air for 8 h to give a dark green solution. $NaClO_4 \cdot H_2O$ (350 mg, 2.0 mmol) in H_2O (20 mL) was added, and the solution was concentrated by a rotary evaporator until cloudy. Allowing the mixture to stand overnight under air at room temperature resulted in the formation of dark green prismatic crystals (which had sufficient quality for X-ray crystallography). The crystals were collected by filtration, washed with water, and dried in a vacuum. Yield: 116 mg (0.15 mmol, 60%). Mp: >300 °C. ^{1}H NMR (CD_3CN), δ: 8.71 (1H, br), 8.69 (2H, s), 8.60 (2H, d, J = 5 Hz), 8.44 (2H, d, J = 8 Hz), 8.19 (2H, t, J = 8 Hz), 7.73 (1H, s), 7.67 (1H, d, J = 8 Hz), 7.61 (3H, m), 7.32 (2H, m), 7.28 (1H, d, J = 8 Hz), 6.90 (1H, s), 6.81 (1H, d, J = 7 Hz), 6.79 (1H, s), 6.51 (1H, t, J = 8 Hz), 4.04 (2H, t, J = 6 Hz), 3.54 (3H, s), 2.83 (2H, m), 1.48 (2H, m), 1.03 (2H, m). UV−vis−NIR (CH_3CN), λ_{max}/nm (ϵ/M^{-1} cm^{-1}): 450 (350), 688 (180), 1410 (10), 1907 (90). IR (KBr), ν/cm^{-1}: 623, 658, 746, 760, 799, 1109, 1217, 1250, 1420, 1438, 1464, 1475, 1549, 1616, 2949, 3074, 3231, 3423. ESI-MS (CH_3CN), m/z: 671 ([Co(**1a**)(1-MeIm)]$^+$), 589 ([Co(**1a**)]$^+$). Anal. Calcd for $C_{36}H_{34}N_6O_9ClCo$ (**2a**·H_2O): C, 54.80; H, 4.34; N, 10.65. Found: C, 54.98; H, 4.39; N, 10.96.

[Co(1b)(1-MeIm)]ClO_4 (2b). This compound was prepared similarly to **2a**. Mp: >300 °C. ^{1}H NMR (CD_3CN), δ: 8.83 (2H, s), 8.68 (1H, br), 8.58 (2H, d, J = 5 Hz), 8.47 (2H, d, J = 8 Hz), 8.19 (2H, t, J = 8 Hz), 7.71 (1H, d, J = 9 Hz), 7.66 (1H, s), 7.61 (3H, m), 7.24 (3H, m), 6.89 (1H, s), 6.84 (1H, d, J = 7 Hz), 6.74 (1H, s), 6.50 (1H, t, J = 8 Hz), 4.15 (2H, m), 3.53 (3H, s), 2.81 (2H, m), 1.80 (2H, m), 1.19 (2H, m), 1.08 (2H, m). UV−vis−NIR (CH_3CN), λ_{max}/nm (ϵ/M^{-1} cm^{-1}): 450 (380, shoulder), 686 (210), 1410 (10), 1907 (90). IR (KBr), ν/cm^{-1}: 623, 660, 752, 770, 1107, 1219, 1248, 1241, 1439, 1458, 1477, 1545, 1618, 1638, 2860, 2920, 3423. ESI-MS (CH_3CN), m/z: 685 ([Co(**1b**)(1-MeIm)]$^+$), 603 ([Co(**1b**)]$^+$). Anal. Calcd for $C_{37}H_{34}N_6O_8ClCo$: C, 56.61; H, 4.37; N, 10.70. Found: C, 56.89; H, 4.38; N, 11.17.

[Co(1c)(1-MeIm)]ClO_4 (2c). This compound was also prepared similarly to **2a**. Mp: >300 °C. ^{1}H NMR (CD_3CN), δ: 8.88 (2H, s), 8.64 (1H, br), 8.59 (2H, d, J = 5 Hz), 8.46 (2H, d, J = 8 Hz), 8.21 (2H, t, J = 8 Hz), 7.76 (1H, d, J = 8 Hz), 7.63 (4H, m), 7.28 (3H, m), 6.90 (1H, d, J = 8 Hz), 6.84 (1H, s), 6.65 (1H, s), 6.52 (1H, t, J = 8 Hz), 4.18 (2H, t, J = 5 Hz), 2.87 (2H, q, J = 7 Hz), 1.79 (2H, m), 1.29 (2H, m), 1.10 (2H, m), 0.92 (2H, m). UV−vis−NIR (CH_3CN), λ_{max}/nm (ϵ/M^{-1} cm^{-1}): 450 (400, shoulder), 682 (240), 1407 (10), 1908 (90). IR (KBr), ν/cm^{-1}: 623, 657, 735, 762, 793, 1107, 1217, 1252, 1420, 1439, 1460, 1547, 1618, 2930, 3441. ESI-MS (CH_3CN), m/z: 699 ([Co(**1c**)(1-MeIm)]$^+$), 617 ([Co(**1c**)]$^+$). Anal. Calcd for $C_{38}H_{38}N_6O_9ClCo$ (**2c**·H_2O): C, 55.86; H, 4.69; N, 10.28. Found: C, 55.76; H, 4.63; N, 10.33.

X-ray Structure Determinations. In each case, cell constants and intensity data were collected at 293 K on a Rigaku AFC5S diffractometer equipped with a molybdenum sealed tube (λ(Mo Kα) = 0.710 69 Å, 50 kV 25 mA) and with a graphite monochromator. The data were corrected for Lorentz−polarization effects, and an empirical absorption correction based on a ψ scan was applied. Three standard reflections monitored every 150 reflections showed no decay in intensity. The structures were solved by direct methods and refined on F by full-matrix least-squares techniques; all calculations were performed with the TEXSAN[23] crystallography software package from the Molecular Structure Corp. Atomic scattering facters were taken from ref 24. All non-hydrogen atoms were refined anisotropically. Hydrogen atoms were fixed at calculated positions, except for the amide hydrogen (labeled H(1) for both structures), which was located by a difference Fourier synthesis and refined isotropically. The final R values (calculated for the observed reflections), as well as other crystallographic parameters, are listed in Table 1.

Computational Methods. The quantum chemical calculations were carried out with the Gaussian-98[25] set of programs running on a Silicon Graphics Origin 2000 workstation. The geometry optimization was performed at the Hartree−Fock level using double-ζ basis sets (LANL2DZ).

Acknowledgment. We thank Dr. Kiyoshi Tsuge (Institute for Molecular Science) for assistance with the X-ray crystallography and a number of helpful suggestions. We are also grateful to Ms. Sachiyo Nomura (Institute for Molecular Science) for performing elemental analyses, to Professor Atsuhiro Osuka (Kyoto University) for permission to use the JEOL HX-110 mass spectrometer, to Professor Yoshihito Watanabe and Dr. Seiji Ogo (Institute for Molecular Science) for assistance with the ESI-MS measurements, and to Dr. Hajime Ito (Institute for Molecular Science) for assistance with the Gaussian-98 calculations.

Supporting Information Available: Tables of complete atomic coordinates and isotropic thermal parameters, anisotropic thermal parameters, bond lengths, and bond angles for complexes **1a** and **1b** (Tables A−J), ORTEP views of the complex cations in **1a** and **1b** with complete numbering schemes (Figure A), optimized structures of the two stereoisomers of [Co(2,6-pyridinedicarboxaldimine)(O=$CHCH_2O$-(1−))(NH_3)]$^+$ (Figure B), and text giving characterization data for **1b**, **1c**, and precursor compounds. This material is available free of charge via the Internet at http://pubs.acs.org.

IC9912880

(23) *TEXSAN: Crystal Structure Analysis Package*; Molecular Structure Corp.: The Woodlands, TX, 1985, 1992.
(24) *International Tables for X-ray Crystallography*; Kynoch Press: Birmingham, England, 1974.
(25) Frisch, M. J.; Trucks, G. W.; Schlegel, H. B.; Scuseria, G. E.; Robb, M. A.; Cheeseman, J. R.; Zakrzewski, V. G.; Montgomery, J. A., Jr.; Stratmann, R. E.; Burant, J. C.; Dapprich, S.; Millam, J. M.; Daniels, A. D.; Kudin, K. N.; Strain, M. C.; Farkas, O.; Tomasi, J.; Barone, V.; Cossi, M.; Cammi, R.; Mennucci, B.; Pomelli, C.; Adamo, C.; Clifford, C.; Ochterski, J.; Petersson, G. A.; Ayala, P. Y.; Cui, Q.; Morokuma, K.; Malick, D. K.; Rabuck, A. D.; Raghavachari, K.; Foresman, J. B.; Cioslowski, J.; Ortiz, J. V.; Stefanov, B. B.; Liu, G.; Liashenko, A.; Piskorz, P.; Komaromi, I.; Gomperts, R.; Martin, R. L.; Fox, D. J.; Keith, T.; Al-Laham, M. A.; Peng, C. Y.; Nanayakkara, A.; Gonzalez, C.; Challacombe, M.; Gill, P. M. W.; Johnson, B.; Chen, W.; Wong, M. W.; Andres, J. L.; Gonzalez, C.; Head-Gordon, M.; Replogle, E. S.; Pople, J. A. *Gaussian-98*, Revision A.5; Gaussian, Inc.: Pittsburgh, PA, 1998.